Parity violating electron scattering off nuclei: excitation of the discrete spectrum

S. Pastore, G. Co'

Dipartimento di Fisica, Università di Lecce

and

Istituto Nazionale di Fisica Nucleare,

sezione di Lecce,

I-73100 Lecce, Italy

A. M. Lallena

Departamento de Fisica Moderna,

Universidad de Granada,

E-18071 Granada, Spain

Abstract

We study the nuclear excitation to discrete states induced by parity violating electron scattering experiments. The sensitivity of the results to the uncertainties related to the nucleon form factors is investigated. Results of calculations for the ^{208}Pb nucleus are presented.

PACS numbers: 25.30.-c;25.30.Dh;13.40.Gp

I. INTRODUCTION

The advances of the last decade in the experimental techniques, have transformed parity-violating electron scattering (PVES) from an exotic discussion topic to a well established part of the research program at a variety of accelerator facilities. The physics that PVES can explore, can be roughly divided in three main areas: test of standard model of electroweak interactions, investigation of nucleon properties and study of nuclear structure. Testing the standard model has been the basic motivation of the experiments done up to now, on deuteron [1], ^{9}Be [2] and ^{12}C [3] nuclear targets. From the theoretical point of view, the opportunities offered by PVES to get information on the nucleon form factors [4, 5] and also on its strange quark contents [6, 7] have been widely studied. Also the possibility of obtaining information on the neutron distribution in the nuclear ground state has been thoroughly investigated [8–10].

The main attention of the theoretical PVES studies has been addressed to elastic scattering or to the excitation of the quasi-elastic peak. In this paper we investigate the physics of the PVES when discrete states are excited. The major objection done so far to this kind of experiment is related to the small values of the unpolarized cross sections with respect to those of the elastic and quasi-elastic regimes [4]. We have verified that, for a fixed value of the momentum transfer, our cross sections are usually one order of magnitude smaller than those of the quasi-elastic peak. The situation is certainly challenging but not hopeless.

On the other hand, the excitation of the discrete states has various advantages with respect to the elastic and quasi-elastic scattering. Since there is the possibility of selecting a specific excitation mode with its angular momentum and parity, it is possible to probe separately the various responses acting on electric and magnetic transitions. In addition, the nucleus is not destroyed and all the complications related to the final state interactions between emitted particles and rest nucleus are not present.

In section II we briefly recall the basic expressions related to PVES. The main emphasis of the paper is on the applications. We have chosen to study a specific doubly magic nucleus: ^{208}Pb. This choice has been motivated by the fact that this nucleus presents a rich discrete spectrum, which has been well studied from the experimental point of view. In section III we first present our description of the excited states structure, based upon the Random Phase Approximation (RPA), and then the results we have obtained. A summary of the work and the conclusions can be found in section IV.

II. FORMALISM

In this section we briefly describe the derivation of the cross section expression for the process of inclusive scattering of polarized electrons from nuclei. We assume that the polarization of the electron is known, but we do not consider the eventual polarization of the nucleus. We work in natural units ($\hbar = c = 1$) and in the ultrarelativistic regime for the electron, therefore we neglect the terms proportional to its mass. The electron wave functions, before and after the scattering process, are plane wave solutions of the Dirac equation. The transition amplitude of the process is given by the sum of the electromagnetic and weak amplitudes. Each term is calculated by contracting the corresponding leptonic and hadronic tensors [5].

The currents produced by the nucleus are described within the traditional approach used for the scattering of unpolarized electrons. We fix the quantization axis along the direction of the momentum transfer $\mathbf{q}$, and perform a multipole expansion of the four-currents. Then we define the multipole operators of longitudinal type,

$$M^{\alpha}_{J0}(q) = \int \mathrm{d}^3 r\, j_J(qr)\; Y_{J0}(\theta,\phi)\; J^0_\alpha(\mathbf{r}) \;, \tag{1}$$

$$L^{\alpha}_{J0}(q) = \frac{i}{q}\int \mathrm{d}^3 r\; \{\nabla\left[j_J(qr)\; Y_{J0}(\theta,\phi)\right]\}\cdot \mathbf{J}_\alpha(\mathbf{r}) \;, \tag{2}$$

and of transverse type,

$$T^{\alpha,\mathrm{E}}_{J\lambda}(q) = \frac{1}{q}\int \mathrm{d}^3 r\; \left\{\nabla\times\left[j_J(qr)\,\mathbf{Y}^{\lambda}_{JJ}(\theta,\phi)\right]\right\}\cdot \mathbf{J}_\alpha(\mathbf{r}) \;, \tag{3}$$

$$T^{\alpha,\mathrm{M}}_{J\lambda}(q) = \int \mathrm{d}^3 r\, j_J(qr)\; \mathbf{Y}^{\lambda}_{JJ}(\theta,\phi)\cdot \mathbf{J}_\alpha(\mathbf{r}) \;, \tag{4}$$

where the z-axis projection λ can assume the values ± 1. In the above equations we have defined $q = |\mathbf{q}|$ and we have indicated with $j_J(qr)$ the spherical Bessel function, with Y_{JM} the spherical harmonics and with $\mathbf{Y}^{M}_{JJ}$ the vector spherical harmonics [11]. The index α of the nuclear four-currents $(J^0, \mathbf{J})$, selects the electromagnetic (em) or the neutral weak current (nc). The upper indexes E and M in the transverse operators indicate, respectively, the electric and the magnetic type of operators.

We consider that the nucleus makes a transition between states of well defined angular momentum and parity. The transition amplitude can be written as:

$$\mathcal{M} \; = \; \langle \Psi_{J_f M_f} | \mathcal{O}_J | \Psi_{J_i M_i} \rangle \; , \tag{5}$$

with

$$\begin{aligned}
\mathcal{O}_J \; = \; & \frac{e^2}{\omega^2 - q^2} \left\{ \sqrt{4\pi} \sum_J i^J \sqrt{2J+1} \, [l_0^{\rm em} M_{J0}^{\rm em} - l_3^{\rm em} L_{J0}^{\rm em}] + \right. \\
& \left. - \sqrt{2\pi} \sum_{J \geq 1} i^J \sqrt{2J+1} \sum_{\lambda = \pm 1} l_\lambda^{\rm em} \left[T_{J\lambda}^{\rm em,E} + \lambda T_{J\lambda}^{\rm em,M} \right] \right\} + \\
- & \frac{G}{2\sqrt{2}} \left\{ \sqrt{4\pi} \sum_J i^J \sqrt{2J+1} \, [l_0^{\rm nc} M_{J0}^{\rm nc} - l_3^{\rm nc} L_{J0}^{\rm nc}] + \right. \\
& \left. - \sqrt{2\pi} \sum_{J \geq 1} i^J \sqrt{2J+1} \sum_{\lambda = \pm 1} l_\lambda^{\rm nc} \left[T_{J\lambda}^{\rm nc,E} + \lambda T_{J\lambda}^{\rm nc,M} \right] \right\} .
\end{aligned} \tag{6}$$

In the above expression the l's indicate the leptonic terms, e the elementary charge, G the Fermi constant and ω the energy transfer.

The cross section is obtained by calculating the modulus squared of the amplitude (6). This means that all the terms in Eq. (6) interfere. We neglect the terms proportional to G^2 since, in the energy regime we consider, their contributions are very small in comparison to those of the other terms.

Because of the V-A character of the weak current the corresponding four-vector operator can be decomposed in vector and axial vector terms, which have opposite behaviour under the action of parity operator. This means that the neutral current operators defined in Eqs. (1)-(4) can be written as:

$$M_{J0}^{\rm nc}(q) \; = \; M_{J0}^{\rm V}(q) + M_{J0}^{\rm A}(q) \; , \tag{7}$$

$$L_{J0}^{\rm nc}(q) \; = \; L_{J0}^{\rm V}(q) + L_{J0}^{\rm A}(q) \; , \tag{8}$$

$$T_{J\lambda}^{\rm nc,E}(q) \; = \; T_{J\lambda}^{\rm V,E}(q) + T_{J\lambda}^{\rm A,E}(q) \; , \tag{9}$$

$$T_{J\lambda}^{\rm nc,M}(q) \; = \; T_{J\lambda}^{\rm V,M}(k) + T_{J\lambda}^{\rm A,M}(q) \; . \tag{10}$$

We show in Table I the parity of the various multipole operators we have to consider. Even though the operators ($M_{J0}^{\rm em}$,$M_{J0}^{\rm V}$,$L_{J0}^{\rm em}$,$L_{J0}^{\rm V}$) and ($T_{J\lambda}^{\rm em,E}$,$T_{J\lambda}^{\rm V,E}$, $T_{J\lambda}^{\rm A,M}$) have the same parity, they do not interfere. This because the transverse operators T have z-axis projection $\lambda = \pm 1$, while the remaining operators have z-axis projection equal to zero. This implies that these two classes of operators populate final states with different M_f and, therefore, they cannot interfere. Analog reasons prohibit the interference between the ($M^{\rm A}_{J0}$,$L^{\rm A}_{J0}$) operators and the transverse operators ($T^{\rm em,M}_{J\lambda}$,$T^{\rm V,M}_{J\lambda}$,$T^{\rm A,E}_{J\lambda}$). Obviously there is not interference between operators with different parity.

Using the conservation of the electromagnetic current and the Conserved Vector Current hypothesis, we express the longitudinal term of the electromagnetic current and of the vector part of the neutral current as a function of the Coulomb and Coulomb-like terms:

$$L^{\alpha}_{J0}(q) \;=\; \frac{\omega}{q}\, M^{\alpha}_{J0}(q)\,, \qquad \alpha = {\rm em}, {\rm V}\,. \tag{11}$$

The evaluation of the hadron and lepton tensors contraction with the approximations above discussed allows us to write the following expression for the cross section:

$$\begin{aligned} \frac{1}{\sigma_M}\left(\frac{{\rm d}\sigma}{{\rm d}\Omega}\right)^h \;&=\; \left[v_{\rm L} R_{\rm L}\,(q) + v_{\rm T} R_{\rm T}\,(q)\right] \\ &\quad - (c_{\rm V} + h c_{\rm A})\,\frac{G\,|q^2|}{2\pi\alpha\sqrt{2}}\, Re\left[v_{\rm L} R^{\rm V}_{\rm L}\,(q) + v_{\rm T} R^{\rm V}_{\rm T}\,(q) + h v_{\rm T'} R^{\rm A}_{\rm T'}\,(q)\right]\,, \end{aligned} \tag{12}$$

with σ_M the Mott cross section, $c_{\rm A} = 1$, $c_{\rm V} = -1 + 4\sin^2\theta_W \sim 0.092$ and h the helicity of the incoming electron. The v's are terms coming from the leptonic vertex and depending only from kinematics variables:

$$v_{\rm L} \;=\; \frac{(\omega^2 - q^2)^2}{q^4}\,, \tag{13}$$

$$v_{\rm T} \;=\; \tan^2\frac{\theta}{2} - \frac{\omega^2 - q^2}{2q^2}\,, \tag{14}$$

$$v_{\rm T'} \;=\; \tan\frac{\theta}{2}\sqrt{\tan^2\frac{\theta}{2} - \frac{\omega^2 - q^2}{q^2}}\,, \tag{15}$$

where θ is the scattering angle.

The information on the nuclear currents are contained in the R terms defined as:

$$R_{\rm L}\,(q) \;=\; \frac{4\pi}{2J_i + 1}\sum_J \left|\left\langle \Psi_{J_f}\, \| M^{\rm em}_J(q) \|\, \Psi_{J_i}\right\rangle\right|^2\,, \tag{16}$$

$$R_{\rm T}\,(q) \;=\; \frac{4\pi}{2J_i + 1}\sum_{J\,\geq 1}\left[\left|\left\langle \Psi_{J_f}\,\left\| T^{\rm em,E}_J(q)\right\|\,\Psi_{J_i}\right\rangle\right|^2 + \left|\left\langle \Psi_{J_f}\,\left\| T^{\rm em,M}_J(q)\right\|\,\Psi_{J_i}\right\rangle\right|^2\right] \tag{17}$$

and

$$
\begin{aligned}
R^{\rm V}_{\rm L}\left(q\right) &= \frac{2\pi}{2J_i+1}\sum_J \left\langle \Psi_{J_f}\left\|M^{\rm em}_J(q)\right\|\Psi_{J_i}\right\rangle \left\langle \Psi_{J_f}\left\|M^{\rm V}_J(q)\right\|\Psi_{J_i}\right\rangle^* , & (18)\\
R^{\rm V}_{\rm T}\left(q\right) &= \frac{2\pi}{2J_i+1}\sum_{J\ \geq 1}\left[\left\langle \Psi_{J_f}\left\|T^{\rm em,E}_J(q)\right\|\Psi_{J_i}\right\rangle \left\langle \Psi_{J_f}\left\|T^{\rm V,E}_J(q)\right\|\Psi_{J_i}\right\rangle^*\right. \\
&\quad \left. + \left\langle \Psi_{J_f}\left\|T^{\rm em,M}_J(q)\right\|\Psi_{J_i}\right\rangle \left\langle \Psi_{J_f}\left\|T^{\rm V,M}_J(q)\right\|\Psi_{J_i}\right\rangle^*\right] , & (19)\\
R^{\rm A}_{\rm T'}\left(q\right) &= \frac{2\pi}{2J_i+1}\sum_{J\ \geq 1}\left[\left\langle \Psi_{J_f}\left\|T^{\rm em,M}_J(q)\right\|\Psi_{J_i}\right\rangle \left\langle \Psi_{J_f}\left\|T^{\rm A,E}_J(q)\right\|\Psi_{J_i}\right\rangle^*\right. \\
&\quad \left. + \left\langle \Psi_{J_f}\left\|T^{\rm em,E}_J(q)\right\|\Psi_{J_i}\right\rangle \left\langle \Psi_{J_f}\left\|T^{\rm A,M}_J(q)\right\|\Psi_{J_i}\right\rangle^*\right] . & (20)
\end{aligned}
$$

In the above equation we imply that the angular part of the matrix element should be evaluated as reduced matrix element.

The asymmetry is defined as the ratio of the difference between the cross sections with different helicity h and their sum. Using Eq. (12) we find for the asymmetry the following expression:

$$
\mathcal{A} = -\mathcal{A}_0 \frac{c_{\rm A}\left[v_{\rm L}R^{\rm V}_{\rm L}\left(q\right) + v_{\rm T}R^{\rm V}_{\rm T}\left(q\right)\right] + c_{\rm V}v_{\rm T'}R^{\rm A}_{\rm T'}\left(q\right)}{v_{\rm L}R_{\rm L}\left(q\right) + v_{\rm T}R_{\rm T}\left(q\right)} , \tag{21}
$$

where we have defined

$$
\mathcal{A}_0 = \frac{G(q^2-\omega^2)}{2\pi\alpha\sqrt{2}} . \tag{22}
$$

For the kinematics we are interested to investigate $\mathcal{A}_0$ is of the order of 10^{-6}.

In this kind of experiments only the parity-violating part of the weak current interaction can be measured. Eq. (12) shows that also a parity-conserving weak current term is present, but it is masked by the electromagnetic term at our energies. The only way of disentangling this term is to use neutrinos as a probe.

The single nucleon currents are constructed with the common procedure of using the on-shell nucleon currents and making a non-relativistic reduction [6]. The multipole operators are:

$$
\begin{aligned}
M^{\rm em}_{J0}\left(q\right) \;&=\; \sum_{i=1}^{A} G^{\tau}_{\rm E}\left(q^2\right)\, j_J\left(qr_i\right)\, Y_{J0}\left(\theta_i,\phi_i\right)\,, \qquad (23)\\
T^{\rm em,E}_{J\lambda}\left(q\right) \;&=\; \sum_{i=1}^{A}\left[-\frac{G^{\tau}_{\rm E}\left(q^2\right)}{M_\tau}\sum_{s=\pm1}\frac{s\sqrt{J+\delta_{s,-1}}}{\hat{J}}\, j_{J+s}\left(qr_i\right)\,\mathbf{Y}^{\lambda}_{J+s,J}\left(\theta_i,\phi_i\right)\cdot\nabla_i\right.\\
&\qquad\left.+\,q\,\frac{G^{\tau}_{\rm M}\left(q^2\right)}{M_\tau}\, j_J\left(qr_i\right)\,\mathbf{Y}_{JJ}\left(\theta_i,\phi_i\right)\cdot\boldsymbol{\sigma}_i\right]\,, \qquad (24)\\
T^{\rm em,M}_{J\lambda}\left(q\right) \;&=\; \sum_{i=1}^{A}\left[-i\,\frac{G^{\tau}_{\rm E}\left(q^2\right)}{M_\tau}\, j_J\left(qr_i\right)\,\mathbf{Y}^{\lambda}_{JJ}\left(\theta_i,\phi_i\right)\cdot\nabla_i\right. \qquad (25)\\
&\qquad\left.-i\,q\,\frac{G^{\tau}_{\rm M}\left(q^2\right)}{2M_\tau}\sum_{s=\pm1}\frac{s\sqrt{J+\delta_{s,-1}}}{\hat{J}}\, j_{J+s}\left(qr_i\right)\,\mathbf{Y}^{\lambda}_{J+s,J}\left(\theta_i,\phi_i\right)\cdot\boldsymbol{\sigma}_i\right]
\end{aligned}
$$

where τ is the index that distinguishes between protons (p) and neutrons (n), and M_τ is the nucleon mass.

The vector terms of the weak current have the same analytic expression of the electromagnetic ones, the only difference is in the nucleon form factors. The electromagnetic form factors $G^{\tau}_{\rm E,M}$, should be substituted with [6]:

$$
G^{\rm V,(p,n)}_{\rm E,M} \;=\; (1-4\sin^2\theta_W)\, G^{\rm (p,n)}_{\rm E,M} - G^{\rm (n,p)}_{\rm E,M} + G^{\rm s}_{\rm E,M} \qquad (26)
$$

where we have indicated with $G^{\rm s}_{\rm E,M}$ the contribution of the strange quark.

For the axial currents we find the expressions:

$$
T^{\rm A,E}_{J\lambda}\left(q\right) \;=\; \sum_{i=1}^{A}\frac{1}{q}\, G^{\tau}_{\rm A}\left(q^2\right)\int {\rm d}\mathbf{r}\,\left[j_J\left(qr_i\right)\,\mathbf{Y}^{\lambda}_{JJ}\left(\theta_i,\phi_i\right)\right]\cdot\nabla\times\boldsymbol{\sigma}_i\,\delta\left(\mathbf{r}-\mathbf{r}_i\right) \qquad (27)
$$

and

$$
T^{\rm A,M}_{J\lambda}\left(q\right) \;=\; \sum_{i=1}^{A} G^{\tau}_{\rm A}\left(q^2\right)\, j_J\left(qr_i\right)\,\mathbf{Y}^{\lambda}_{JJ}\left(\theta_i,\phi_i\right)\cdot\boldsymbol{\sigma}_i\,, \qquad (28)
$$

where $G^{\tau}_{\rm A}$ is the axial-vector form factor of the nucleon.

Since one of the aims of our work is to study the sensitivity of the asymmetry to the nucleon form factors, we shall discuss with some detail our choices of the various parameterizations. Our basic choice of the electromagnetic form factors is based upon the parameterization given in [12]. For comparison we have also used the more common dipole parameterization:

$$
G^{\rm p}_{\rm E} = G^{\rm D}_{\rm V}\,; \quad G^{\rm n}_{\rm E} = 0\,; \quad G^{\rm p}_{\rm M} = \mu_{\rm p} G^{\rm D}_{\rm V}\,; \quad G^{\rm n}_{\rm M} = \mu_{\rm n} G^{\rm D}_{\rm V}\,, \qquad (29)
$$

where

$$G_{\rm V}^{\rm D} = \left[1 + \frac{q^2 - \omega^2}{M_{\rm D}^2} \right]^{-2} , \tag{30}$$

with $M_{\rm D} = 842$ MeV and $\mu_{\rm p}$ and $\mu_{\rm n}$ the proton and neutron magnetic moments.

For the axial-vector form factor we use a dipole expression:

$$G_{\rm A}^{(\rm p,n)} = \mp g_{\rm A} \left[1 + \frac{q^2 - \omega^2}{M_{\rm A}^2} \right]^{-2} \tag{31}$$

where the minus sign refers to the proton and the plus sign to the neutron. In our calculations we used $g_{\rm A}$=1.262, taken from the neutron β decay, and $M_{\rm A}$=1 GeV. We shall discuss the sensitivity of our results to the axial-vector current by changing the values of $g_{\rm A}$ and $M_{\rm A}$ within the range of the uncertainty given by the various measurements of these quantities. Concerning the strange form factors we follow the choice done in [6].

III. APPLICATIONS

The formalism presented in the previous section, has been applied to the ^{208}Pb nucleus. The motivations of this choice have been presented in the introduction. We describe the excited states of the nucleus by using the discrete Random Phase Approximation (RPA) approach developed by the Jülich group [13–15]. This approach provides a reasonable description of the inclusive electron scattering cross section [16, 17]. This means that the shapes of the measured cross sections are rather well described. Usually the RPA cross sections require a quenching factor to reproduce the data. The theoretical interpretation of this fact is still debated [18]. Since asymmetries are ratios of cross sections, we believe that the quenching problem would not be relevant for our purposes.

In our RPA calculations the single particle states are generated by diagonalizing a single particle hamiltonian with a Woods-Saxon potential in a harmonic oscillator basis. The parameters of the potential are taken from Ref. [14] and have been fixed to reproduce the empirical single particle energies around the Fermi surface. The configuration space is composed by all the states below the Fermi level and by the particle states up to five major harmonic oscillator shells. The highest single particle orbit has $l = 9$ and $j = 17/2$.

To evaluate the sensitivity of our results to the nuclear model, we made RPA calculations with two different effective nucleon-nucleon interactions. A first one is a zero-range force of

Landau-Migdal type:

$$V_{\rm LM}(1,2) \;=\; C_0\;[f_0(\rho) \;+\; f_0'(\rho)\,\boldsymbol{\tau}_1\cdot\boldsymbol{\tau}_2 \;+\; g_0\,\boldsymbol{\sigma}_1\cdot\boldsymbol{\sigma}_2 \;+\; g_0'\,\boldsymbol{\sigma}_1\cdot\boldsymbol{\sigma}_2\,\boldsymbol{\tau}_1\cdot\boldsymbol{\tau}_2]\;\delta(\mathbf{r}_1-\mathbf{r}_2)\,, \quad (32)$$

where the parameters f_0 and f_0' have a linear dependence on the nuclear density ρ:

$$f(\rho(r)) \;=\; f^{ext} \;+\; \left(f^{ext}-f^{int}\right)\,\frac{\rho(r)}{\rho(0)} \qquad (33)$$

where r is the distance from the center of the nucleus. The calculations done with this interaction will be labeled as RPA-LM.

The second interaction we have used is the Jülich-Stony Brook one [15]. This force is constructed by adding two finite-range terms describing the exchange of pion and rho mesons, to a zero-range part of Landau-Migdal type. The calculations done with this second interaction would be labeled as RPA-JSB.

In Table II we give the values of the f's and g's parameters used in our calculations. The value of the C_0 constant in Eq. (32) is 386 MeV fm^3. For both forces these parameters have been fixed to reproduce the excitation energy of the collective low lying 3^- state of ^{208}Pb at 2.65 MeV.

We have applied our formalism to the 3^- state and to other rather collective states. In these cases the uncertainties related to the nuclear structure description are larger than the possible effects we wished to disentangle. For this reason we have concentrated our attention to the high-spin states where few particle-hole (p-h) configurations contribute to the excitation. We discuss separately the results obtained for the magnetic and electric excitations.

A. Magnetic states

In the excitation of the magnetic states the $R_{\rm L}$ and $R_{\rm L}^{\rm V}$ terms of the asymmetry, Eq. (21), do not contribute. We discuss the results obtained for the two 12^- states at 6.43 MeV and 7.06 MeV. The two main p-h transitions exciting these two states are the neutron $\mathrm{n}(1j_{15/2}1i^{-1}_{13/2})$ and proton $\mathrm{p}(1i_{13/2}1h^{-1}_{11/2})$ transitions. The 6.43 MeV state is neutron dominated, while the other state is proton dominated. Our RPA calculations clearly show this structure, but they add, to the two main components, other 24 p-h excitations with very small amplitude. We have studied the sensitivity of our results to the details of the description of the excited states by considering also a simple model where only the two main p-h components above mentioned have been considered. The calculations done within this simple model are labeled -st. The values of the X amplitudes of the two main p-h transitions in all cases are given in Table III.

In Fig. 1 we show the responses corresponding to the excitation of the two 12^- states considered, when polarized electrons are used. These responses are presented as a function of the momentum transfer. The $R_{\rm T}$ responses are compared with the data of Ref. [19]. The three calculations maintain their characteristics in all the responses. For the 6.43 MeV state, the RPA-JSB results are always the smallest ones while the RPA-LM are the largest ones. Their role is interchanged for the 7.06 MeV state. The relative behaviour of the responses is strictly related to the values of the X amplitudes as it is evident from Table III.

We show in Fig. 2 the asymmetries calculated with the responses of Fig. 1. The asymmetries, Eq. (21), depend upon the scattering angle θ through the $v_{\rm T}$ and $v_{\rm T'}$ coefficients. For each excited state we show asymmetries for three values of the scattering angle. The meaning of the lines is the same as in Fig. 1.

The order of magnitude of the asymmetries is the expected one: 10^{-6}. All the lines show the same trend: the asymmetries increase in absolute value with increasing q. The shapes are rather smooth and do not present the feature of the responses which are instead well peaked around q=2 fm^{-1}. The curious behavior of the asymmetries above q=2.5 fm^{-1} is produced by the deep minima of our responses. In principle these minima are zero, since we work in plane wave Born approximation. They are not exactly zero because of the discretization of the q values in our calculations. A more refined treatment of the process would require a description of the electron wave functions in terms of wave distorted by the nuclear Coulomb potential. This would produce responses without such a deep minima [8].

The shapes of the asymmetries are not deeply modified by the change of the scattering angle. We notice that the asymmetries of the neutronic 12^- state, the one at 6.43 MeV, is slightly more sensitive to the nuclear model than that of the protonic state.

We have studied the contribution of the various current terms involved in the calculations. From the electromagnetic point of view we realized that both states are dominated by the magnetization current terms. The contribution of the convection current is two order of magnitude smaller. More interesting is the role played by the vector and axial-vector currents in the asymmetry. We show in Fig. 3 the results obtained in RPA-JSB calculations when the weak vector current, dotted lines, and the axial vector current, dashed lines, are respectively switched off. For sake of an easy comparison we show again with the full lines the results of the complete RPA-JSB calculations.

The weak vector current appears in the $R^{\rm V}_{\rm T}$ term, Eq. (19), while the axial vector current appears in the $R^{\rm A}_{\rm T'}$ term (20).The contribution of this term is also depleted by the c_V factor. The figure show analogous trends for both 12^- states. The weak vector current is the main source of the asymmetry, and strongly dominates on the axial term. The contribution of the axial term increases with increasing θ. This is related to the kinematic factor $v_{\rm T'}$ (15) which is directly proportional to $\tan\theta/2$. This specific dependence upon θ could have been used in disentangle the effects of the axial vector current. Unfortunately its contribution is too small to believe to be detectable.

We have also investigated the effects on the asymmetries produced by the uncertainties of 15% on the axial properties of the nucleon. Since the contribution of the axial current is so small, it is evident that there is no detectable sensitivity to uncertainties on the axial mass, or on $g_{\rm A}$. Also the modifications of the nucleon form factors due to the presence of strange quarks in the nucleon do not produce changes in the asymmetries above the threshold of the numerical accuracy of the calculations.

B. Electric state

All the responses in the cross section, Eq. (12), contribute to the excitation of electric states. The study of the asymmetries is in principle more complicated than in the case of the magnetic states. We summarize the results of our investigation by discussing the excitation of a 10^+ state at 5.92 MeV and a 12^+ state at 6.10 MeV.

The inclusive cross sections calculated with RPA-JSB (full lines) and RPA-LM (dotted lines) models, are compared in Fig. 4 with the data of Ref. [19]. The X amplitudes of the two main *p-h* configurations are given in Table IV. The 10^+ is an admixture of a neutron and proton *p-h* configurations, while the 12^+ excitation is essentially due to a single neutron configuration with a small contamination of another neutron *p-h* component.

To test the sensitivity of the result to the details of the description of the excitation, we have calculated the cross sections with a simple two-state model, whose amplitudes are also given in Table IV. The results obtained with this simple model are shown in Fig. 4 by the dashed lines.

In general, the two RPA calculations produce results which are rather similar in all cases. However, the two-state model gives rise to cross sections which differ from the RPA ones with the exception of the 10^+ state for $\theta = 90^o$. In this case all calculations practically coincide. The source of this beheviour is related to the transverse electromagnetic response $R_{\rm T}$. At 90^o the longitudinal response still dominates the cross section, therefore the difference is relatively small. At 160^o the cross section is dominated by the transverse response and the difference becomes more evident. The $R_{\rm T}$ responses are dominated by the magnetization current. The presence of small p-h amplitudes in the RPA builds up a contribution of the magnetization current which is larger than that of the two-state model. The dependence of the asymmetries from the nuclear structure model is shown in Fig. 5. The results are very similar for all the models considered.

In Fig. 6 we show the role of the vector and axial-vector weak currents. The full lines are the RPA-JSB asymmetries shown in Fig. 5. The dotted lines have been obtained by leaving out the weak vector current, while the dashed lines have been obtained without the axial current. As we found in the magnetic excitations, also here the contribution of the axial currents is very small, therefore there is no hope to use polarized electron scattering experiments to investigate the nucleon axial form factors.

We have also investigated the sensitivity of our results to the choice of the electromagnetic form factor. This sensitivity is very small for the magnetic states, but it could be relevant for the electric states; at least for certain kinematics. We show in Fig. 7 the RPA-JSB asymmetries for the 12^+ state calculated with the form factors of [12], full lines, and with the dipole parameterization (29), dashed lines. The changes of the nucleon form factors produce effects larger than those due to the nuclear structure uncertainty.

The differences in the asymmetries are produced by the electric neutron form factor $G_{\rm E}^{\rm n}(q)$, which is zero in the dipole parameterization. We have tested the sensitivity of the asymmetry to $G_{\rm E}^{\rm n}(q)$ by making a calculation with the form factors of Ref. [12], reducing $G_{\rm E}^{\rm n}(q)$ by half. The results of this calculation are shown by the dotted lines. Since the 12^+ is almost a pure neutronic excitation, the strength of $R_{\rm L}$ is due to $G_{\rm E}^{\rm n}(q)$. At forward angles, the kinematic factor $v_{\rm L}$ dominates over $v_{\rm T}$ and $v_{\rm T'}$, then the asymmetries are ruled by the $R_{\rm L}$ and $R_{\rm L}^{\rm V}$ responses, which are very sensitive to $G_{\rm E}^{\rm n}(q)$. The effect disappears with increasing θ, where the transverse responses dominate.

IV. CONCLUSIONS

In this paper we have investigated the opportunities offered by PVES experiments to investigate nucleon and nuclear properties when the nuclear discrete spectrum is excited. We have presented results obtained for the doubly magic nucleus ^{208}Pb. Of its rich spectrum we have investigated only non-collective excitations where the nuclear structure description is better kept under control. For the magnetic excitations we show results for two 12^- states while for the electric excitations we considered a 10^+ and a 12^+ state. The description of the existing unpolarized data requires a quenching of our theoretical cross sections. We believe that this problem is not relevant in the study of the asymmetries which are defined as cross sections ratios.

In all the cases we have studied the contribution of the axial vector current is very small. This drops any hope of studying the nucleon axial form factors. Also the effects produced by the strange content of the nucleon are irrelevant for the observables we have considered.

We found the possibility of obtaining information on the electric form factor of the neutron $G_{\rm E}^{\rm n}(q)$. This is not a common feature of this kind of experiments, but it is a characteristic of the 12^+ state. The excitation of this state, is essentially produced by a pure neutronic *p-h* transition, therefore the electromagnetic longitudinal transition amplitude is dominated by $G_{\rm E}^{\rm n}(q)$. At small scattering angles the asymmetries are dominated by the longitudinal responses. The effects obtained by modifying the $G_{\rm E}^{\rm n}(q)$ form factor, we took from [12], are noticeably larger than the eventual uncertainties in the nuclear structure description of the 12^+ excitation. From the experimental point of view this is a challenging experiment, since a knowledge of the cross sections with few percent accuracy is required.

---

[1] C. Y. Prescott *et al.*, Phys. Lett. **B77**, 347 (1978).

[2] W. Heil *et al.*, Nucl. Phys. **B327**, 1 (1989).

[3] P. A. Souder *et al.*, Phys. Rev. Lett. **65**, 694 (1990).

[4] M. J. Musolf and T. W. Donnelly, Nucl. Phys. **A546**, 509 (1992).

[5] M. J. Musolf, T. W. Donnelly, J. Dubach, S. J. Pollock, S. Kowalski, and E. J. Beise, Phys. Rep. **239**, 1 (1994).

[6] J. E. Amaro, J. A. Caballero, T. W. Donnelly, A. M. Lallena, E. Moya de Guerra, and

J.M. Udías, Nucl. Phys. **A602**, 263 (1996).

[7] W. M. Alberico, S. M. Bilenky, and C. Maieron, Phys. Rep. **358**, 227 (2002).

[8] C. J. Horowitz, Phys. Rev. C **57**, 3430 (1998).

[9] T. W. Donnelly, J. Dubach, and I. Sick, Nucl. Phys. **A503**, 589 (1989).

[10] C. J. Horowitz, S. J. Pollock, P. A. Souder, and R. Michaels, Phys. Rev. C **63**, 025501 (2001).

[11] A. R. Edmonds, *Angular Momentum in Quantum Mechanics* (Princeton University Press, Princeton, 1957).

[12] G. Hoeler *et al.*, Nucl. Phys. **B116**, 505 (1976).

[13] J. Speth, E. Werner, and W. Wild, Phys. Rep. **33**, 127 (1977).

[14] G. Rinker and J. Speth, Nucl. Phys. **A306**, 360 (1978).

[15] J. Speth, V. Klemt, J. Wambach, and G. E. Brown, Nucl. Phys. **A343**, 382 (1980).

[16] S. Krewald and J. Speth, Phys. Rev. Lett. **45**, 417 (1980).

[17] G. Co' and A. M. Lallena, Nucl. Phys. **A510**, 139 (1990).

[18] S. Mokhtar, G. Co', and A. M. Lallena, Phys. Rev. C **62**, 067304 (2000).

[19] J. Lichtenstadt, J. Heisenberg, C. N. Papanicolas, C. P. Sargent, A. N. Courtemanche, and J.S. McCarty, Phys. Rev. C **20**, 497 (1979).

TABLE I: Parity of the multipole operators

parity	operators
$(-)^{J}$	$M^{\rm em}_{J0}, M^{\rm V}_{J0}, L^{\rm em}_{J0}, L^{\rm V}_{J0}, T^{\rm em,E}_{J\lambda}, T^{\rm V,E}_{J\lambda}, T^{\rm A,M}_{J\lambda}$
$(-)^{J+1}$	$M^{\rm A}_{J0}, L^{\rm A}_{J0}, T^{\rm A,E}_{J\lambda}, T^{\rm em,M}_{J\lambda}, T^{\rm V,M}_{J,\lambda}$

TABLE II: Parameters of the interactions used in our calculations.

	f_0^{int}	f_0^{ext}	$f_0^{\prime int}$	$f_0^{\prime ext}$	g_0	g_0'
LM	0.2	-2.45	1.5	1.5	0.55	0.7
JSB	0.21	-1.8	0.65	1.65	0.7	0.7

TABLE III: Amplitudes X of the two main p-h configurations of the 12^- states considered.

	E=6.43 MeV		E=7.06 MeV	
	n$(1j_{15/2}1i^{-1}_{13/2})$	p$(1i_{13/2}1h^{-1}_{11/2})$	n$(1j15/2)(1i13/2)^{-1}$	p$(1i13/2)(1h11/2)^{-1}$
RPA-JSB	0.997	0.050	0.049	0.997
RPA-LM	0.981	0.190	0.188	0.980
2-st	0.990	0.100	0.100	0.990

TABLE IV: Amplitudes X of the two main p-h configurations of the 10^+ and 12^+ states considered.

	10^+ E=5.92 MeV		12^+ E=6.10 MeV	
	n$(1i_{11/2}1i^{-1}_{13/2})$	p$(1h_{9/2}1h^{-1}_{11/2})$	n$(1i_{11/2}1i^{-1}_{13/2})$	p$(1l_{15/2}1h^{-1}_{9/2})$
RPA-JSB	-0.804	0.583	0.987	0.151
RPA-LM	0.621	0.762	0.990	0.132
2-st	-0.800	0.600	0.990	0.100

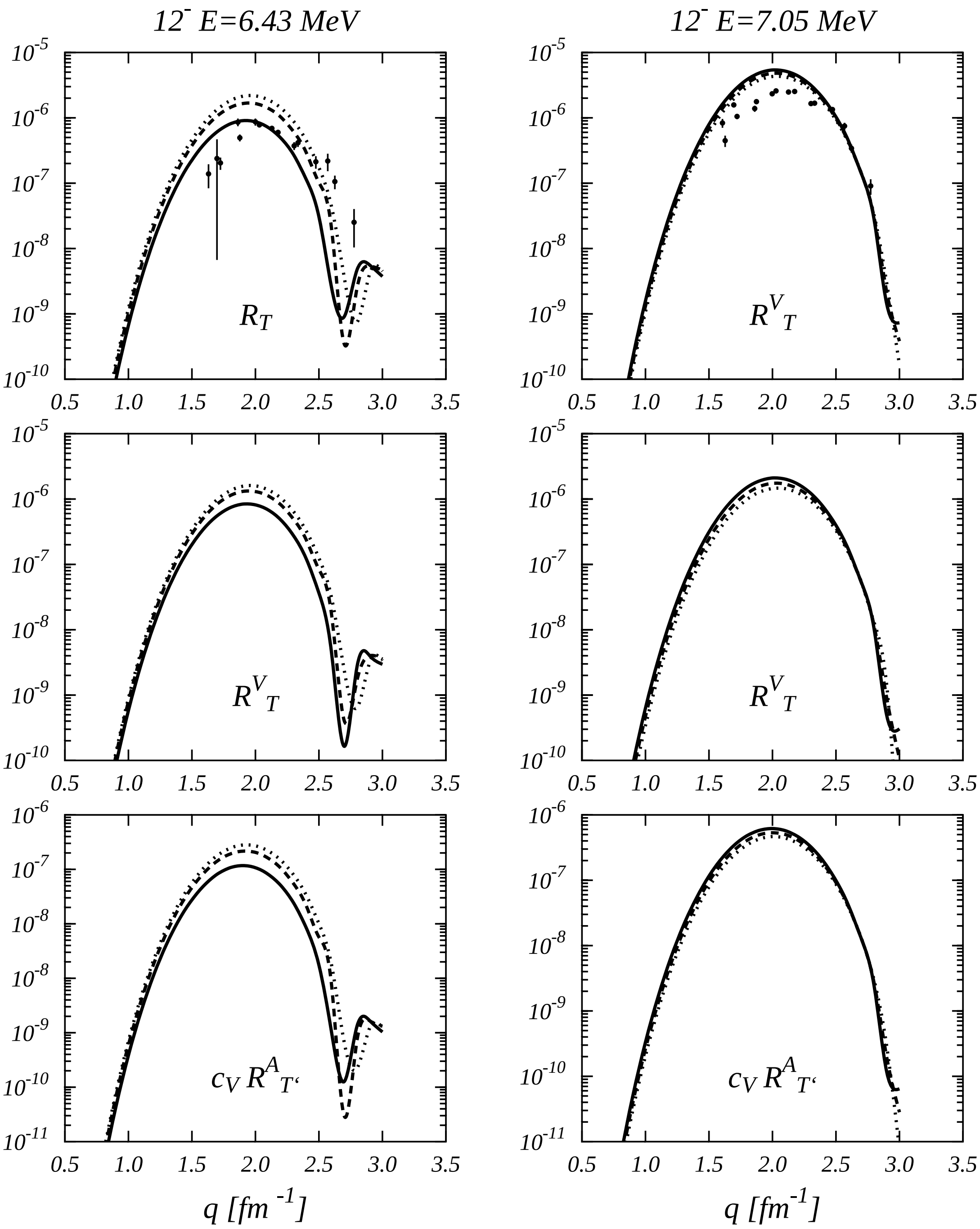

FIG. 1: Responses of the 12^- states considered. The full lines have been obtained with RPA-JSB calculation, the dotted lines with RPA-LM calculation and the dashed lines with the 2-st model. The data are from Ref. [19].

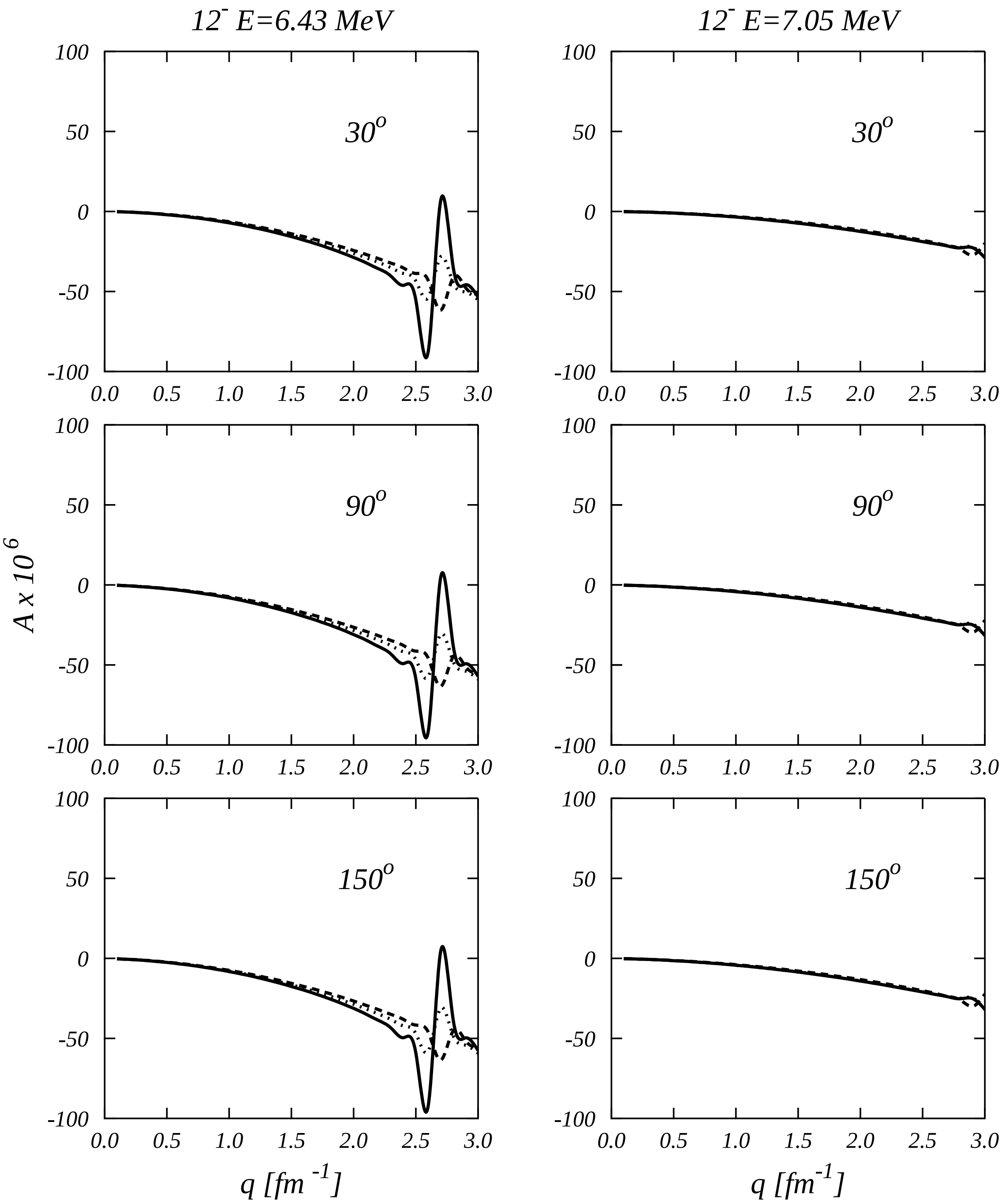

FIG. 2: Asymmetries, multiplied for 10^6, for the 12^- states considered and for three values of the scattering angle. The meaning of the lines is the same as in Fig. 1.

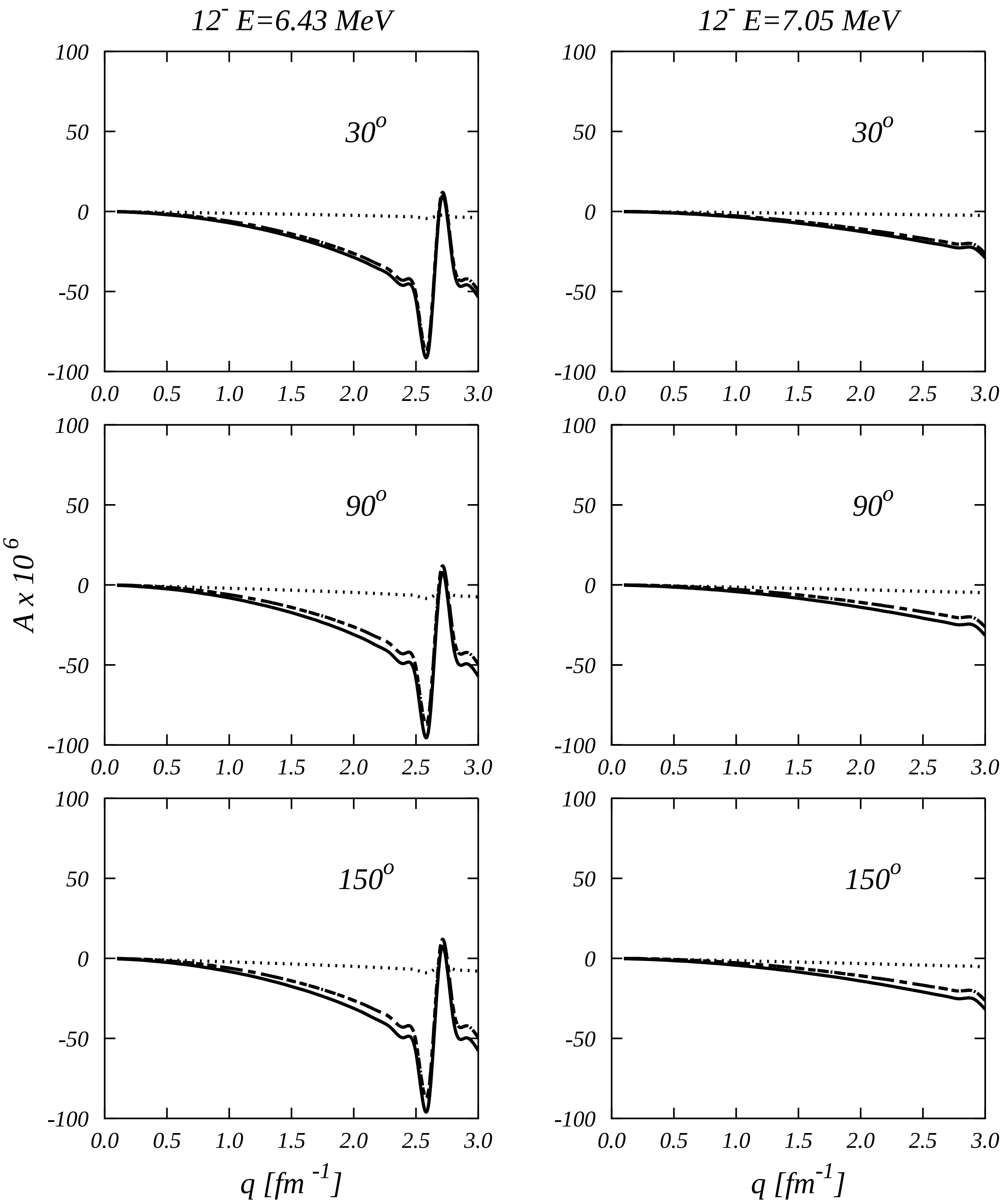

FIG. 3: Asymmetries, multiplied by 10^6, for the 12^- states considered and for three values of the scattering angle. The full lines are the same as in Fig. 2. The dotted lines have been obtained by switching off the weak vector current. The dashed lines by setting to zero the weak axial current.

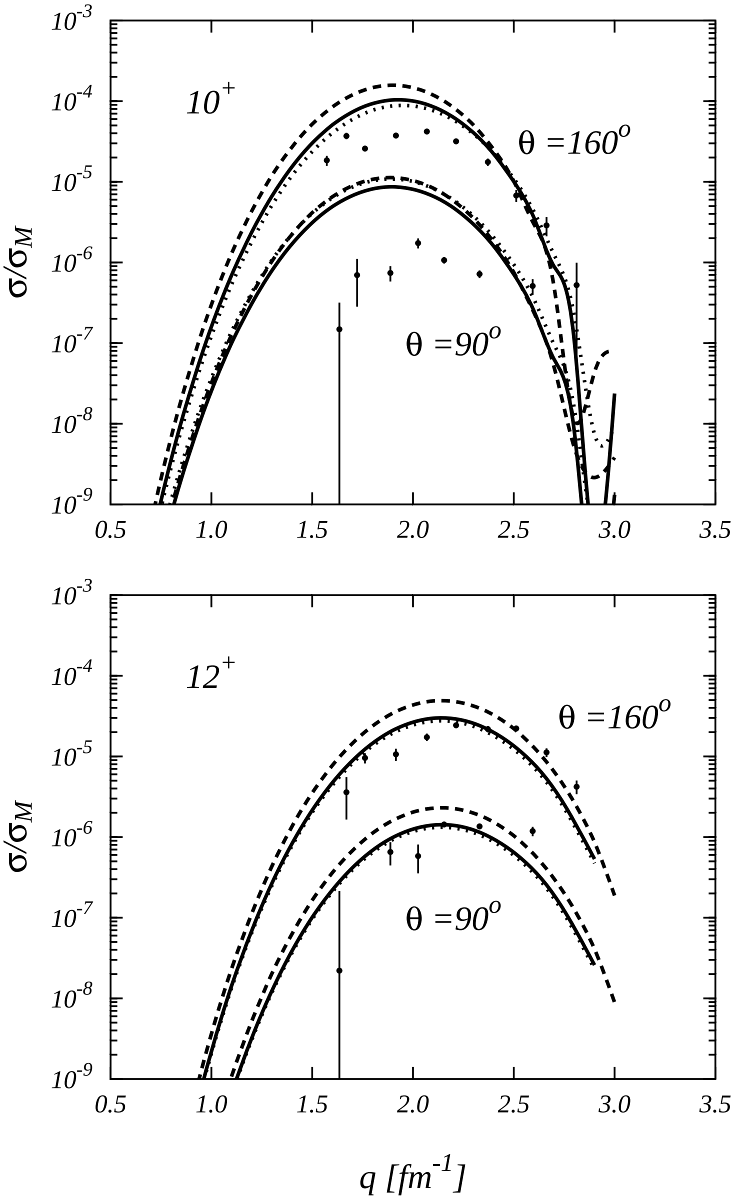

FIG. 4: Cross sections for the 10^+ and 12^+ states considered. The full lines represent the results of RPA-JSB calculations and the dotted lines the RPA-LM results. The dashed lines show the results obtained with the 2-st model. The data are from Ref. [19].

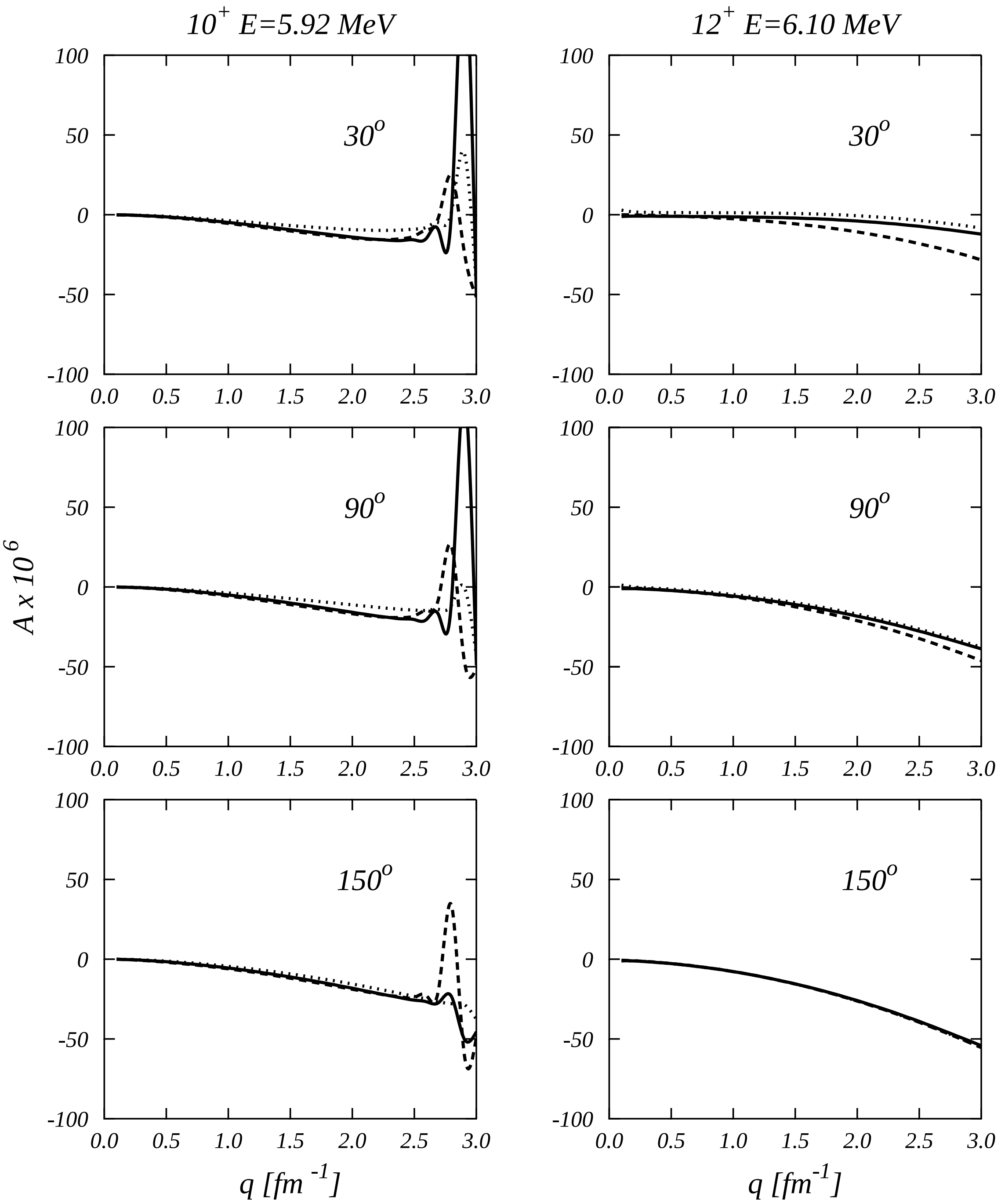

FIG. 5: Asymmetries for the 10^+ and 12^+ states considered. As in Fig. 4 the full and the dotted lines represents the RPA-JSB and the RPA-LM results respectively. The dashed lines show the results of the 2-st model.

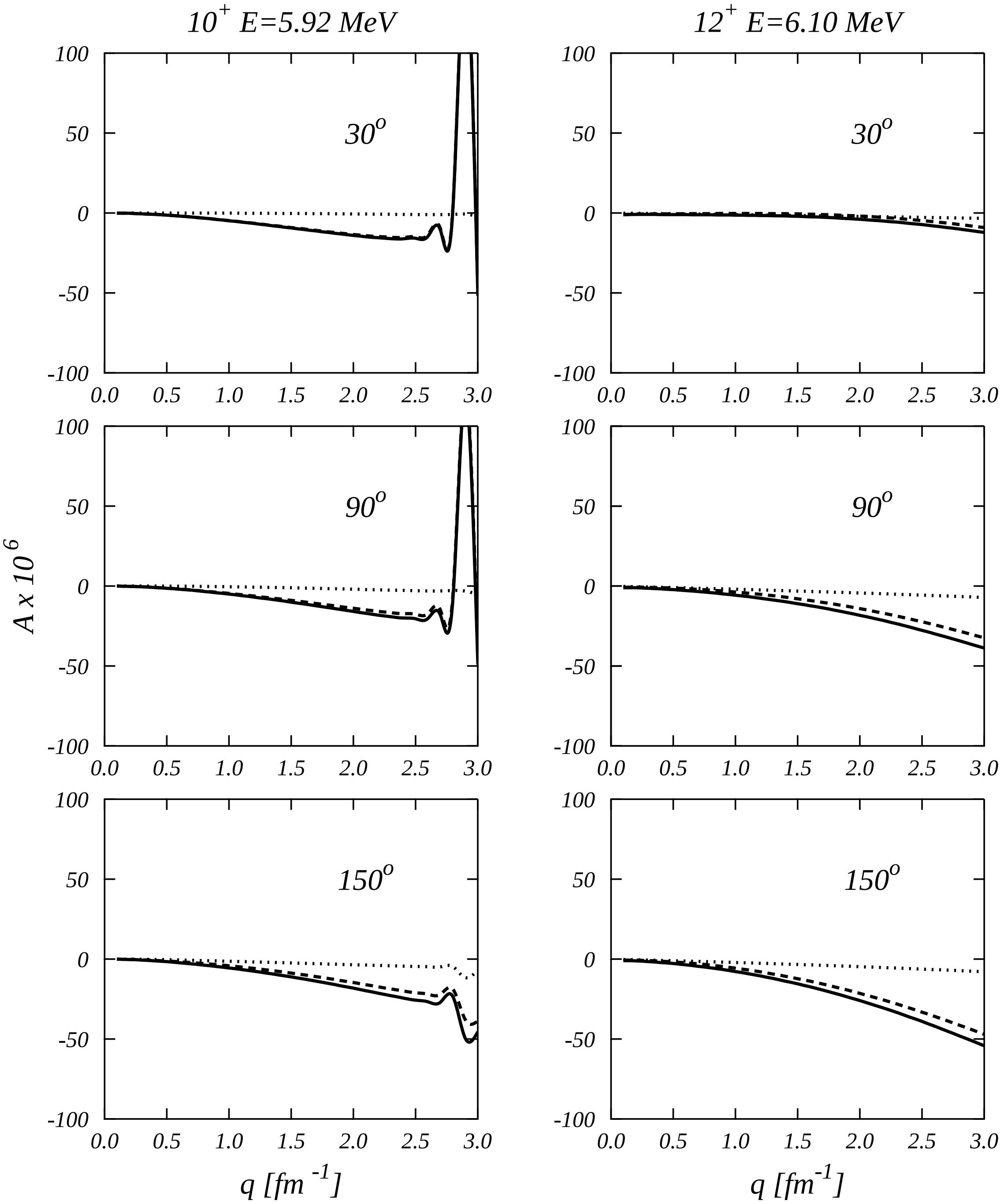

FIG. 6: Asymmetries for the 10^+ and 12^+ states considered. The full lines show the RPA-JSB results, as in Fig. 5. The dotted lines have been obtained without the weak vector currents and the dashed lines without the axial currents.

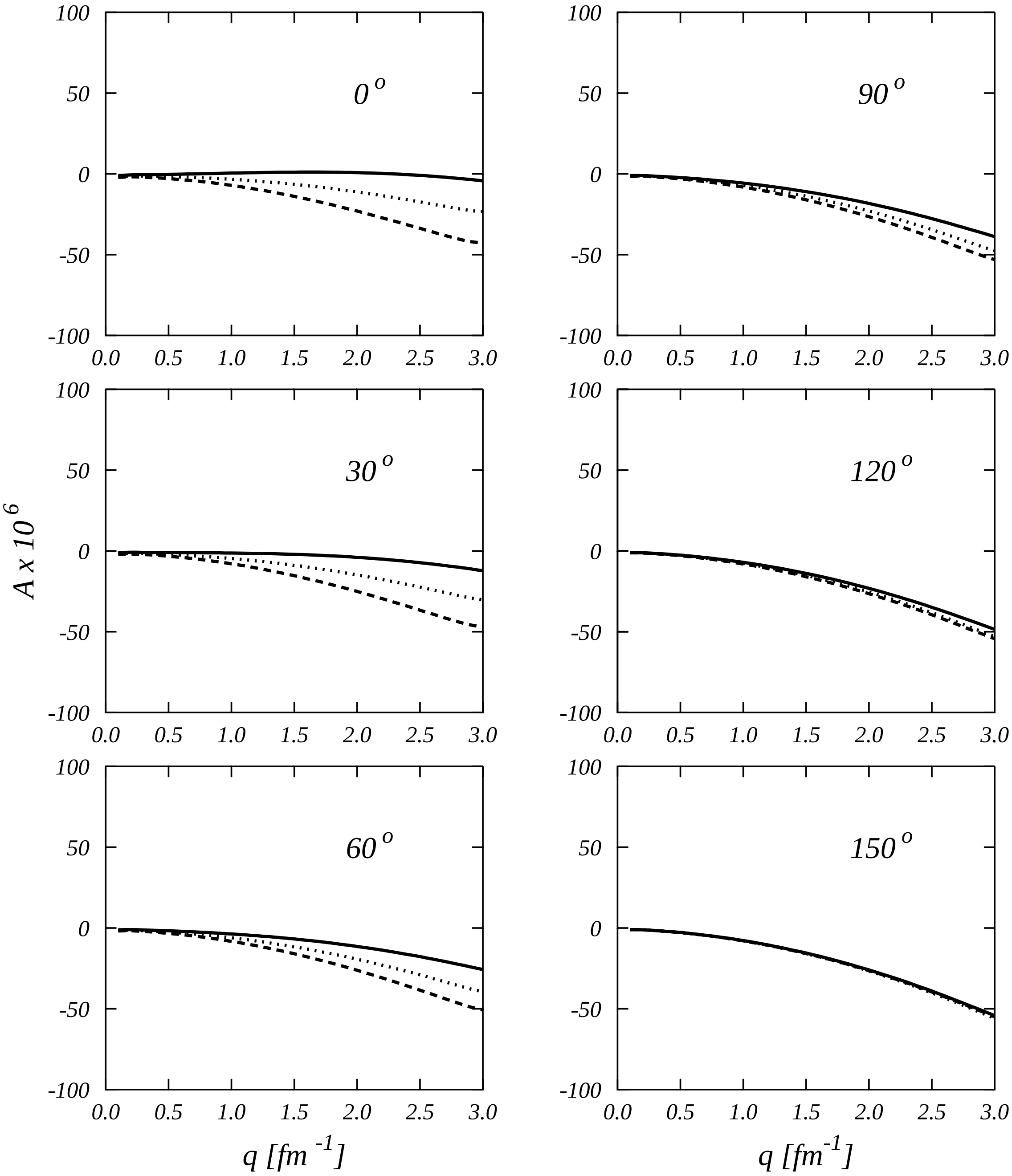

FIG. 7: Asymmetries for the 12^+ at 6.10 MeV. All the curves have been calculated with the RPA-JSB model. The full lines have been obtained with the parameterization of the nucleon electromagnetic form factors taken from [12]. The dashed lines have been calculated using the dipole parameterization. The dotted lines have been obtained with the parameters of Ref. [12] but by dividing by two the value of electric neutron form factor.